Segmentation of Rough Surfaces using Reflectance

G. McGunnigle and M.J. Chantler
Department of Computing and Electrical Engineering
Heriot Watt University
Riccarton
Edinburgh, EH14 4AS, UK
gmg@cee.hw.ac.uk

Abstract

The segmentation of rough surfaces using their reflectance properties is considered. We present a technique to estimate the orientation of surface facets whose reflectance functions are unknown. The reflectance characteristics of each facet are estimated individually allowing this technique to be applied to non-homogeneous surfaces. Non-Lambertian components are attenuated allowing shape estimation with classical photometric stereo. Simulations with rough surfaces rendered with Phong's model indicate that this approach extends the range of reflectance functions to which classical photometric stereo can be applied. The recovered surface derivatives, together with the original intensity images are used to construct reflectance maps. These are used as features for segmentation. A reflectance based classifier is found to be more accurate than an intensity classifier.

1 Introduction

Texture is an important cue for image segmentation. The appearance of a textured surface is a function of its reflectance properties and often the (visible) roughness of the surface. We believe it is both useful and scientifically desirable to resolve these phenomena where possible. In earlier work we have used surface topography as a cue for image segmentation. In this paper we consider the problem of estimating the reflectance characteristics of rough surfaces and using these as a feature for image segmentation. This will, for instance, allow matt and glossy surfaces to be distinguished.

The reflection characteristics of a material can be described using its reflectance map. For a fixed viewing and lighting geometry the intensity of a surface facet is a function of its surface derivatives (p and q). To construct the reflectance map we must first measure the surface derivatives. Photometric stereo is a classical technique to estimate surface derivatives using multiple images of the same scene lit from different directions. It is suitable for rough surfaces because it is local and does not require a smoothness constraint. Most photometric schemes assume the reflectance function is known, e.g. [1]. Recently techniques have been developed to estimate both the surface's topography and

BMVC 2001 doi:10.5244/C.15.34

its reflectance function [2] [3]. We will consider the estimation of shape and reflectance characteristics for image segmentation.

In this paper we will answer two questions: *can we recover the shape of a rough surface whose reflectance characteristics are unknown?* and *is reflectance a useful feature for segmentation?* We propose a novel method for surface estimation and consider some of the issues relevant to segmentation. The method is evaluated using simulation; a rough surface is rendered with realisations of Phong's model and the accuracy of recovery estimated. We test whether the reflectance map is useful for segmentation: a surface is rendered with two realisations of Phong's model and the accuracy of a classifier using reflectance is compared with one using intensity.

We found the proposed algorithm was effective at recovering rough surfaces with a wide range of reflectance characteristics *if* the Lambertian and specular components of the reflectance function are distinctive. Reflectance was found to be a more powerful feature than intensity for image segmentation. We conclude that this is a promising approach for classifying rough surfaces. We believe this paper makes three important contributions. First, a novel technique to attenuate non-Lambertian reflection is proposed; this extends the range of classical photometric stereo. Secondly, the number of photometric images required are expressed in terms of sampling the reflectance function rather than parameterising a model. Thirdly this paper describes the use of the reflectance map for segmentation.

2 General Approach

2.1 Assumptions

We are interested in the recovery of surface derivatives and reflectance functions for the classification and segmentation of test samples. We assume the following experimental set-up, Figure 1. The sample is a rough surface consisting of two or more materials with distinct reflectance characteristics. The rough surface is made up of surface facets which correspond to the image pixels. The slope of a facet is the average slope of the surface in the area corresponding to that pixel. In each image the sample is illuminated by a single light source with azimuth θ. The reflectance functions of the facets, although unknown, do contain a significant Lambertian component. The rough surface is imaged by an overhead camera: an orthographic projection is assumed. The camera is linear and has sufficient dynamic range to accurately measure the range of intensities.

The experiments reported in this paper all use simulation. Despite its drawbacks, simulation is useful in this context for two reasons: first, the correct values of the surface derivatives are known; and secondly it allows a degree of control over the surface reflectance function that would be otherwise impossible. We use Phong's model (Equation 1, [4]) as a benchmark for several reasons: it is simple and is widely used; it has few parameters; the parameters have a clear and direct effect on reflectance. Most importantly, unlike more physical models it does not contain a Gaussian term. Since our empirical model contains a Gaussian term this would undermine the validity of our experimental argument. Essentially, we have chosen the reflectance model that we would expect to least resemble our parametric model.

$$i = K_a + K_d \cos\alpha + K_s \cos^n \gamma \tag{1}$$

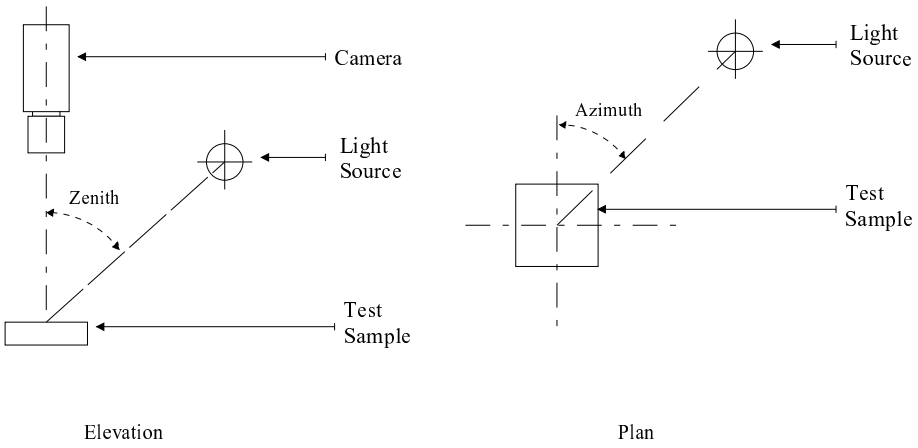

Figure 1: Experimental set-up.

where,

i	is the intensity of the facet.
α	is the angle between the surface normal and the illuminant.
γ	is the angle between the mirror and the viewer directions.
K_a	is the level of ambient radiation (zero in all experiments).
K_d	is the coefficient of diffuse reflection.
K_s	is the coefficient of specular reflection.
n	is the exponent of specular reflection.

2.2 Surface Recovery

To measure the reflectance characteristics of the materials we must first estimate the surface derivatives. Photometric techniques that deal with surfaces with unknown reflectance functions can be grouped into two categories: empirical and analytical. The empirical algorithms assume reflectance is predominantly diffuse and detect and reduce the effects of specular reflection. Coleman and Jain [5] use a simple threshold to detect specularities and use a fourth image for the affected facets. Hansson and Johansson use polarised light to detect and attenuate the specular component of the image [6]. Other investigators have used colour information to detect and suppress specular highlights, e.g. [7]. Analytical schemes estimate both reflectance and shape: they fit a general parametric model of the reflectance map to a data set, then invert the estimated mapping to recover the surface derivatives. Estimating the parameters requires a large data set: schemes either use many lights [3] or assume the surface is homogeneous and estimate a single reflectance function for the entire surface [2].

Our approach is closest to the empirical group—though after surface recovery we use reflectance information for segmentation. Instead of using a two dimensional reflectance map for surface recovery, we treat the reflectance of each surface facet as a one dimensional function of illuminant azimuth. Azimuth functions for particular facets can be

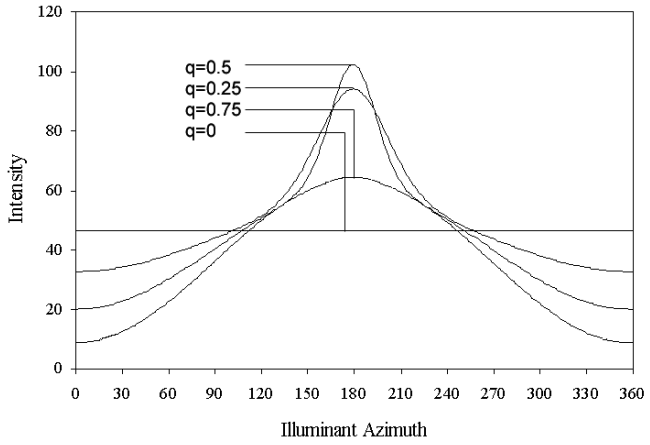

Figure 2: Plot of the azimuth function for surface facets with p=0 and q=0, 0.25, 0.5 and 0.75, rendered with Phong's model, Diffuse coefficient=50, Specular Coefficient=50, Specular exponent=20.

plotted, Figure 2. We model this function as a combination of a Lambertian component and a residue which is due to specular reflection. In this paper our approach is to measure the azimuth function, identify and suppress the residual term, and use the remaining Lambertian term for classical photometric stereo.

2.3 Segmentation

Once we have estimated the orientation of the facets it is possible to construct a series of reflectance maps and segment the image. Other authors have used reflectance as a cue for segmentation and object recognition. Nayar and Bolle present a technique that uses a single image to calculate the reflectance ratios of regions and their backgrounds [8]. Their approach is valid for curved surfaces if the region and its background share scaled versions of the same reflectance function. Our technique, which is designed for more constrained environments, uses multiple images taken under controlled lighting and is able to distinguish between surfaces that differ in the *type* of reflectance characteristic as well as in albedo. This paper describes exploratory work carried out with simulation to assess whether surface estimation is practical and whether the reflectance map is useful for segmentation.

3 Estimating The Azimuth Function

We assume that the residue is normally distributed with azimuth; we justify this on two grounds. First, the surface microtopography of a facet will perturb the direction of the reflected rays. Specular radiation will be distributed across azimuth with a peak at the facet's azimuth (assuming the facet has a non-zero gradient). Secondly, the measured azimuth function is the convolution of the actual function with the angular distribution

Slope (q)	Fundamental	First	Second	Third
0	0.01	0.01	0.01	0.01
0.25	22.69	8.95	5.81	3.37
0.50	28.70	7.56	6.24	4.94
0.75	27.53	0.29	0.13	0.17

Table 1: Strength of the harmonics for facets of various slopes

of the light source. Even if it is not itself Gaussian, a light source of finite extent will cause the measured function to tend towards normality, by the central limit theorem. The Lambertian component of the azimuth function consists of a cosine term and a mean term: the Gaussian component can be decomposed into a Fourier series. The combined function is shown in Equation 2.

$$i(\theta) = a\cos(\theta - \phi) + b + c(1 + 2\sum_{h=1}^{\infty} x^{h^2}\cos(h\theta - h\phi)) \tag{2}$$

where,

$i(\theta)$	is the azimuth function.
θ	is the illuminant azimuth.
ϕ	is the azimuth of the facet.
a,b,c and x	are constants.
h	is the number of harmonic.

Before fitting a model to the azimuth function we must sample the function—that is we must illuminate the surface from a set of directions. Since we treat each facet individually we must sample at enough points not only to estimate the parameters, but also to avoid aliasing effects. By Nyquist, the Lambertian component requires more than two sample points for complete reconstruction. The Gaussian component is a converging series: the number of samples needed will depend on the quality required, the parameters of the Gaussian and the angular distribution of the light source. In Table 1 we show the strength of the harmonics of each of the curves shown in Figure 2. As is evident from the figure, the facets with q=0.25 or 0.5 have significant harmonics corresponding to the specular component.

In order to demonstrate the effect of aliasing we conduct the following simulation: a sphere is rendered with Phong's model. The azimuth function of each facet is sampled at k points, i.e. each facet is illuminated in turn from k directions. The Fourier series of each azimuth function is calculated, and the value of the azimuth function at $\theta = 0°$is reconstructed from the Fourier coefficients, (top row of Figure 3). When k is large, the function is well sampled and the image can be accurately reconstructed. As k is decreased aliasing effects occur and the reconstruction gets progressively worse.

Because the intensity of the light source has an angular distribution, the light source acts as an anti-aliasing filter. The experiment is repeated in the bottom row of Figure 3 with a light source that has a Gaussian distribution with standard deviation 20°. Aliasing effects now occur at much lower sampling rates than previously.

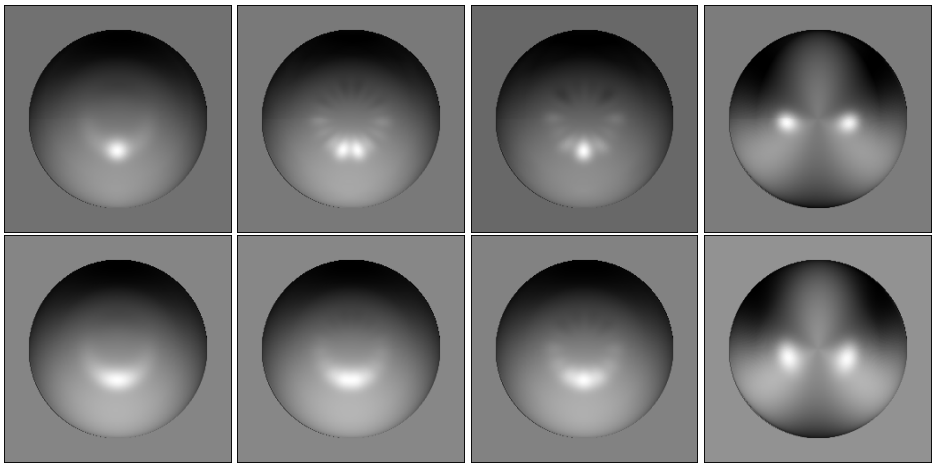

Figure 3: Effect of varying the sampling frequency with point source (top row) and extended souce (bottom row).
Diffuse coefficient = 40, Specular Coefficient=50, Specular exponent n=50, Illuminant zenith = 45°,
Number of samples: 40, 10, 8, 2

4 Surface Recovery

To use classical photometric stereo we must reduce the non-Lambertian component of intensity. Unfortunately the Lambertian and Gaussian function components are not orthogonal: a simple filtering will remove the harmonics due to the Gaussian but will not resolve the Lambertian and residue contributions to the fundamental and mean. We estimate the parameters of the Gaussian: x can be found from the ratio of the first and second harmonics, this allows c to be determined and the Gaussian reconstructed. The Gaussian's contribution to the fundamental and mean can then be identified and removed.

This approach is successful if the specular component is narrow and distinct from the Lambertian component. If the higher harmonics are small, i.e. the specular lobe is either wide or weak, then the algorithm approximates the Lambertian component with a wide Gaussian. This leads to spurious results when the algorithm removes this estimate from the fundamental and mean components. To avoid these artefacts we introduced a threshold: if the first harmonic was less than a fraction d of the fundamental, then the measured fundamental and mean components were assumed to be due to the Lambertian component and were unaltered before image reconstruction.

We conducted two sets of experiments using simulation. In both experiments we fit our empirical model to the azimuth function of each facet rendered with a standard reflectance model, then estimate the orientation of the facet. An isotropic, random fractal 256×256 surface, with power roll-off β =3.0 and *rms* slope 0.1 was rendered with Phong's model from 360 directions. This level of sampling is excessive and could be reduced for real applications. The algorithm was used to suppress the residual component and photometric stereo was used to estimate the facet slopes. The accuracy of the estimate is compared with that of a surface recovered using the same photometric technique applied

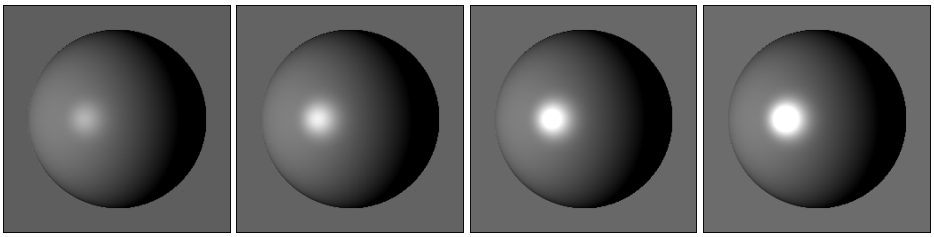

Figure 4: Effect of varying the specular coefficient.
Diffuse coefficient = 50, Specular exponent, n=20, illuminant zenith = 45°,
Specular coefficient=0, 50, 75, 100

to the original data set. In the first experiment the strength of the specular term in Phong's model is varied (Figure 4); in the second the exponent is varied, (Figure 5). We state accuracy in terms of the signal to noise ratio: the ratio of the variance of the p derivative field to the variance of noise—the difference between the correct and estimated field. In both cases the algorithm has generally improved the accuracy of surface recovery, (Figure 6). However, it fails completely when the exponent of the specular term lies between 5 and 20. Below 20 there is insufficient energy in the harmonics; however, below 5, the threshold prevents this type of artefact from being introduced.

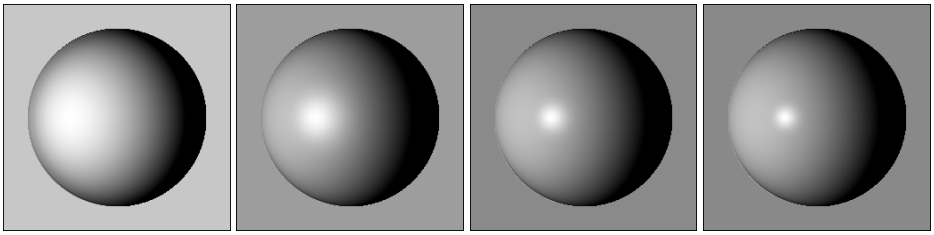

Figure 5: Effect of varying the specular exponent.
Diffuse coefficient = 50, Specular coefficient=20, illuminant zenith = 45°,
Specular exponent, n=0, 20, 30, 50

We stress that these results are exploratory: we have only used simulation allowing us to make some simplifications. First, we assume superposition: i.e. our camera is linear and has sufficient dynamic range to maintain a level of accuracy for photometric recovery. Cameras that fulfil these requirements have recently become widely available. Secondly, in our model we have neglected shadowing; in the simulations we account for self, but not cast, shadows. This assumption limits the roughness of the test surfaces, and the zenith angle from which they can be lit. However, we believe that these results are sufficiently promising to justify further investigation.

5 Segmentation

For a fixed viewing and illumination geometry the intensity, i, of a surface facet is a function of the surface derivatives, p and q and is described by the reflectance map. The

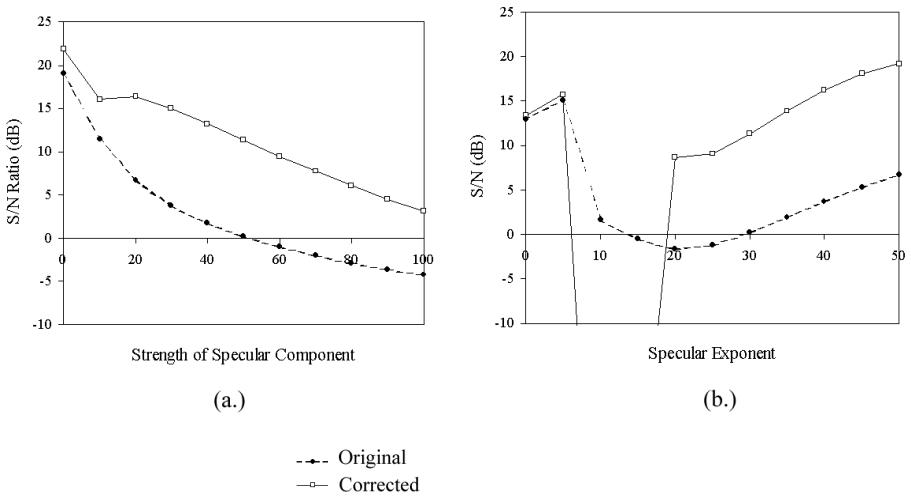

Figure 6: Performance of recovery on original and corrected data.
Diffuse coefficient = 50, d=0.1, illuminant zenith = 45°,
In (a.) Specular exponent, n=20
In (b.) Specular coefficient=20

reflectance map is characteristic of the material: the vector R=[*p,q,i*] is a useful feature set for material classification. Figure 7 shows contour plots of two reflectance maps from different realisations of Phong's model.

By estimating the surface shape we get the vector R at each facet. Both the measured quantity *i* and the estimated quantities *p* and *q* are subject to errors and it is more appropriate to describe the relation as a three dimensional probability distribution, *P(p,q,i)*. Since we are dealing with rough surfaces, *p* and *q* are random variables and follow a statistical distribution. For example, an isotropic, globally flat surface will have a joint distribution of *p* and *q* that is circular and centred on the origin. The feature distribution is the joint distribution of reflectance and slope, *F(p,q,i)*.

Many natural surfaces have a Gaussian distribution of surface derivatives. In the simplest case the reflectance function is linear within the sampling region; the distribution of intensities will also be Gaussian and a simple quadratic discriminant will be optimal. More complex reflectance functions will require more complex discriminants for optimality.

The usefulness of reflectance as a feature was tested. Two rough surfaces with different reflectance functions, but similar topography, must be distinguished. The obvious approach is to low pass filter the image and classify on the averaged intensity. In our simulations a random fractal (power roll-off β=3.0, rms slope =0.1) is rendered with two realisations of Phong's model. An intensity based classifier and a reflectance classifier are used to discriminate between the surfaces. We used a linear, Bayesian, discriminant trained on the test image.

We vary the width of the low pass filter applied to both the intensity and the derivative

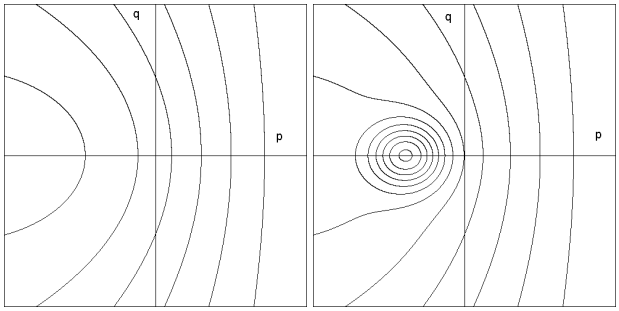

Figure 7: Reflectance maps of two realisations of Phong's model.

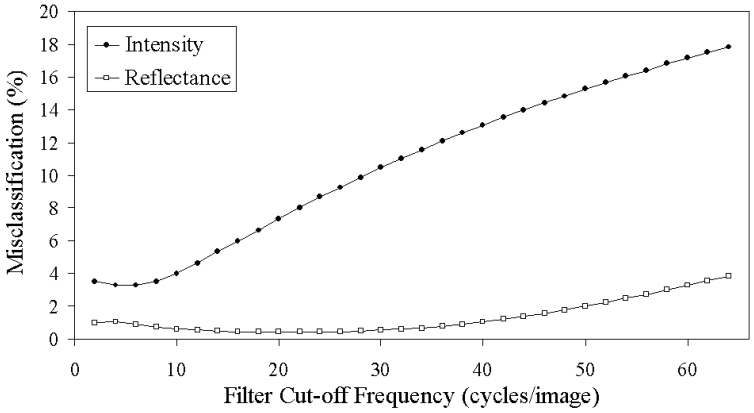

Figure 8: Performance of intensity and reflectance based classifiers.
Texture 1: Diffuse Coefficient 50, Specular Coefficient = 0,
Texture 2: Diffuse Coefficient 50, Specular Coefficient = 50, Specular exponent, 20

fields. Both the intensity and reflectance classifiers show an increase in misclassification as the size of the filter is reduced. However, throughout the experiment the reflectance classifier is significantly more accurate than the intensity classifier, (Figure 8). A segmentation by each of the classifiers, with a low pass filter with cut-off 32 cycles per image, is shown in Figure 9.

6 CONCLUSIONS

This paper is concerned with the use of reflectance to segment rough surfaces. We proposed a method to recover the orientation of facets whose reflectance function is unknown. We also highlighted the issue of aliasing in the estimation process. This technique was found to extend the application of photometric stereo to reflectance functions with non-Lambertian components. Recovery of the surface derivatives allows the construction of a reflectance map. We described the use of the reflectance map as a feature set for segmenting rough surfaces. Our simulations indicate that reflectance is a more powerful

feature than intensity for distinguishing between rough surfaces with different reflectance properties.

References

[1] R.J. Woodham *Photometric Method for Determining Surface Orientation From Multiple Images Optical Engineering Vol.19 No.1, pp.139-144, January/February 1980,*

[2] H. Tagare and R.J. deFigueiredo *Simultaneous Estimation of Shape and Reflectance Maps from Photometric Stereo, Proceedings of the Third International Conference on Computer Vision Osaka, Japan 4-7 Dec. 1990 IEEE Computer Society Press. 1990, pp.340-343. Los Alamitos, CA, USA*

[3] G. Kay and T. Caelli *Estimating the Parameters of an Illumination Model Using Photometric Stereo,* Graphical Models and Image Processing, Vol.571, No.5 September, pp.365-388, 1995

[4] A. Watt *3D Computer Graphics,* Third Edition, Addison-Wesley, 2000

[5] E. N. Coleman and R. Jain *Obtaining 3-dimensional shape of textured and specular surfaces using four source photometry Computer Graphics and Image Processing 18 pp.309-328, 1982*

[6] P. Hansson and P. Johansson *Topography and reflectance analysis of paper surfaces using photometric stereo method Optical Engineering Vol.39 No.9 pp.2555-2561, September 2000*

[7] K. Schlüns and O. Wittig *Photometric Stereo for Non-Lambertian Surfaces Using Color Information*, Proc. 7th Int. Conference on Image Analysis and Processing, Capitolo, Monopoli, Italy, Sept. 20-22, 1993, 505-512.

[8] S.K. Nayar and R.M. Bolle *Reflectance Based Object Recognition, International Journal of Computer Vision 1996*

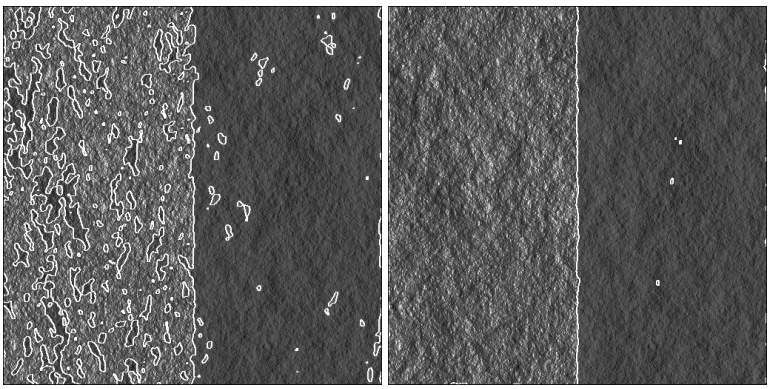

Figure 9: Comparison of segmentations by intensity (left) and reflectance (right).